Published in final edited form as:
J Proteome Res. 2013 October 4; 12(10): . doi:10.1021/pr400688r.

Brain proteomics supports the role of glutamate metabolism and suggests other metabolic alterations in protein L-isoaspartyl methyltransferase (PIMT)-knockout mice

Hongqian Yang[1], **Jonathan D. Lowenson**[2], **Steven Clarke**[2], and **Roman A. Zubarev**[1,3,*]

[1]Division of Physiological Chemistry I, Department of Medical Biochemistry and Biophysics, Karolinska Institutet, Scheeles väg 2, SE-17 177 Stockholm, Sweden

[2]Department of Chemistry and Biochemistry and the Molecular Biology Institute, University of California, Los Angeles, CA 90095, USA

[3]SciLifeLab, Stockholm, Sweden

Abstract

Protein L-isoaspartyl methyltransferase (PIMT) repairs the isoaspartyl residues (isoAsp) that originate from asparagine deamidation and aspartic acid (Asp) isomerization to Asp residues. Deletion of the gene encoding PIMT in mice (*Pcmt1*) leads to isoAsp accumulation in all tissues measured, especially in the brain. These PIMT-knockout (PIMT-KO) mice have perturbed glutamate metabolism and die prematurely of epileptic seizures. To further elucidate the role of PIMT, brain proteomes of PIMT-KO mice and controls were analyzed. The isoAsp levels from two of the detected 67 isoAsp sites (residue 98 from calmodulin and 68 from glyceraldehyde-3-phosphate dehydrogenase) were quantified, and found significantly increased in PIMT-KO mice ($p < 0.01$). Additionally, the abundance of at least 151 out of the 1017 quantified proteins was found to be altered in PIMT-KO mouse brain. Gene Ontology analysis revealed that many down-regulated proteins are involved in cellular amino acid biosynthesis. For example, the serine synthesis pathway was suppressed, possibly leading to reduced serine production in PIMT-KO mice. Additionally, the abundances of enzymes in the glutamate-glutamine cycle were altered towards the accumulation of glutamate. These findings support the involvement of PIMT in glutamate metabolism and suggest that the absence of PIMT also affects other processes involving amino acids synthesis and metabolism.

Keywords

proteomics; tandem mass spectrometry; posttranslational modifications

Introduction

Protein damage is believed to be one of the major processes in aging.[1] Natural proteins are subject to various types of damage, such as oxidation, deamidation and racemization of amino acid residues, as well as misfolding of the polypeptide chain. Although cells containing damaged proteins can be removed by the immune system, the level of damaged proteins within cells can also be reduced via lysosomal or proteasomal degradation or by molecular repair pathways. The protein L-isoaspartyl methyltransferase (PIMT) is a repair enzyme that initiates the conversion of the isoaspartyl residue (isoAsp), which is a major

*Corresponding author: Roman.Zubarev@ki.se, Telephone: +46 8524 87594.

product of protein damage via asparagine (Asn) deamidation and aspartate (Asp) isomerization, to normal Asp residues.[2] The conversion occurs via isoAsp methylation, using S-adenosyl-L-methionine (AdoMet) as the methyl donor, followed by cyclization and hydrolysis.[3] PIMT is a well-conserved enzyme in nature; it is expressed in almost all cells and tissues, and is particularly highly expressed in brain.[4] PIMT-knockout (PIMT-KO) mice show retardation of growth, perturbed glutamate metabolism, and usually die at less than 2 months of age from fatal seizures.[5] As expected, the level of isoAsp-containing proteins increases with time compared to wild type (WT) controls: the abundance of brain isoAsp in 30 to 40-day old PIMT-KO mice reaches around 1200 pmol/mg protein compared to 200 pmol/mg in WT mice.[5] Abnormalities of microtubule organization in the dendrites of pyramidal neurons have also been reported in PIMT-KO mice.[6] As the expression of the PIMT is essential for survival, the substrates of PIMT under physiological conditions have been under intense investigation.[7–11] Because of the strong physiological response, there are reasons to suspect that the PIMT knockout affects important brain pathways.[5, 6] Thus far, it has been reported that PIMT regulates p53 activity,[12] and the absence of the methyltransferase results in activation of the insulin pathway[13, 14] and MEK-ERK[15] pathway. In order to provide a deeper understanding into the molecular changes induced by PIMT deficiency, we performed here proteomics analysis of the whole PIMT-KO mouse brain. The goal of the analysis was two-fold: 1) to examine the effect of PIMT on isoAsp content in previously reported and newly identified PIMT substrates; and 2) to identify proteins with significantly altered abundances and to map them on metabolic pathways.

In previous studies, we have quantified isoAsp content with label-free shotgun proteomics in clinical samples (blood plasma of Alzheimer's disease [AD] patients)[16] and studied brains in an AD mouse model.[17] Here, as in a previous work, we applied a filter-aided in-solution sample preparation (FASP) protocol that successfully deals with the problem of the large lipid content of the brain.[18] Proteomics findings are typically validated by an orthogonal approach, e.g. Western blot or ELISA. However, immunological validation works best when the changes in protein abundances reach the levels of 50% or more, while here we aimed to un-biasedly detect smaller abundance variations. Therefore, to corroborate the findings provided by FASP proteomics, we performed, as in the previous work, an additional proteomics analysis using a different sample preparation method: protein digestion in solution following sample delipidation by gel electrophoresis. Such a validation approach, although not fully orthogonal to the discovery method (mass spectrometry was used in both analyses for protein identification and quantification), is still satisfactory due to the complementary nature of FASP sample preparation compared with gel-based methods. Indeed, the peptides detected with these two approaches are often different, although they originate from the same proteins.[19]

The detection of isoAsp residues has traditionally relied on the immunological assay or PIMT-based enzymatic assay.[20] The recent emergence of electron capture dissociation (ECD) and electron transfer dissociation (ETD) has led to the ability of tandem mass spectrometry (MS/MS) to differentiate isoAsp from Asp residues by a "signature" fragment of (z - 57 Da).[21] However, additional filtering based on evaluation of the tandem mass spectra as well as the chromatography profiles of the eluting peptides is required to reach a high level of specificity in proteome-wide isoAsp analysis.[22, 23] Another problem is *in vitro* isoAsp production. Proteomics sample preparation, especially protein digestion, often induces Asn deamidation, and thus generates isoAsp residues (at moderate levels of 3–5%).[23] At the same time, Asp isomerization leading to isoAsp is a much slower process,[24] and thus it is mostly induced *in vivo*. To track the isoAsp contents introduced in vitro, 18O labeling sample preparation procedure has been developed.[25–27] In the previous study of blood plasma proteins, we only investigated isomerization-produced isoAsp because of the low level of isoAsp in human blood.[16] In the present study, higher levels of isoAsp are

expected in the PIMT-KO mouse brain cells,[4, 5] which reduces the concern over *in vitro* deamidation. Even if some deamidation occurs during sample preparation, a higher level of isoAsp residues at a particular site in a PIMT-KO protein relative to its WT counterpart will indicate that this isoAsp is a physiological substrate of PIMT. Therefore, we investigate here isoAsp residues originating from both deamidation and isomerization processes. Using shotgun proteomics, we have presented the brain isoaspartome for the first time.

Experimental section

PIMT-knockout mice

As described previously, PIMT knockout mice ($Pcmt1^{-/-}$) with a background of 50% C57BL/6 and 50% 129/Sv were generated by breeding heterozygous $Pcmt1^{+/-}$ mice that had been inbred for over fifteen years.[5] These mice were treated in accordance with animal use protocols approved by the UCLA Animal Research Committee (Protocol 1993–109). Eight young female mice (4 $Pcmt1^{-/-}$ and 4 $Pcmt1^{+/+}$; 51 to 53 days old) were decapitated. The brain was removed as quickly as possible, cut in half with a razor blade, and dropped into liquid nitrogen. The frozen brains were then stored at −80 °C until further analysis. Genotyping by PCR was performed both prior to weaning and after dissection to confirm each animal's identification.[5] The sample name, gender, type and age of the mice used are listed in Table S1.

Brain proteome extraction

Protein extraction buffer containing 62.5 mM Tris-HCl (pH 6.8), 2% sodium dodecyl sulfate (SDS), 10 mM dithiothreitol (DTT), and 10% glycerol was added to the tissue corresponding to 10 × wet weight (e.g. 10 μL buffer for 1 mg sample). The tissue samples were vortexed and incubated on ice for 5 min. Then the tissues were homogenized on ice by TissueRuptor (QIAGEN), and sonicated on ice for 2 s with a 1 s pause, with a total sonication time of 100 s. The samples were then incubated for 10 min at 70 °C with a shaking frequency of 1400 Hz. Tissue debris was removed by centrifugation at 16000 ×g for 15 min. The protein concentration for each supernatant was determined by the BCA protein assay (Thermo Scientific Pierce) according to the protocol provided by the producer.

Filter-aided sample preparation (FASP)

Protein extracts were digested with trypsin as described previously.[18] Briefly, 10 μg of tissue sample was reduced for 10 min with 5 mM DTT in 50 mM ammonium bicarbonate (AmBic) solution at 90 °C. Then the entire solution was transferred onto a 30 kDa Nanosep Ultrafiltration device (PALL), and the samples were washed twice with 8 M urea in 50 mM AmBic (UA solution) with centrifugation. Incubation at room temperature in dark with 50 mM iodoacetamide (IAA) in UA solution was used for protein alkylation. Sequencing grade modified trypsin (Promega) was used for protein digestion with an enzyme/substrate ratio of 1:50. The samples were incubated overnight at 40 °C, and the final digests were obtained in a solution of 0.5 M NaCl in 5% formic acid (FA). These solutions were desalted by ZipTip (Millipore), dried by SpeedVac, and stored at −20 °C until further analysis.

SDS-polyacrylamide gel electrophoresis (SDS-PAGE) separation

To eliminate the large lipid content of the brain that otherwise risked contaminating the chromatographic equipment, protein extracts (30 Rg of protein per lane) were separated by NuPAGE Novex Bis-Tris Mini Gels (Invitrogen). After protein separation, the gel was stained with 0.1% Coomassie Brilliant Blue R-250 solution.

Protein in-gel digestion

Each gel lane was cut into 15 pieces of approximately equal size. The gel pieces were incubated in destaining solution (50% acetonitrile (ACN) in 50 mM AmBic solution) at 40 °C for 10 min. After applying the destaining procedure twice, the gel pieces were soaked in 100% ACN and incubated at 40 °C until totally dehydrated. Incubation with 10 mM DTT at 40 °C for 30 min followed by 55 mM IAA at 40 °C for 20 min was used for protein reduction and alkylation. Sequencing grade-modified trypsin (Promega) was used for protein digestion with an enzyme/substrate ratio of 1:10. The samples were incubated overnight at 40 °C. The digestion was stopped by 1% FA, and the digested peptides were extracted by 1% FA in 50% ACN. The samples were then cleaned by ZipTip (Millipore). Samples from the same lane were pooled together, dried by SpeedVac, and treated afterwards as one sample. Dried samples were stored at −20 °C until further analysis.

Mass spectrometry (MS) analysis

Protein digests (0.5 μg, resuspended in 0.1% FA) were loaded into a 25 cm long column (New Objective) home-packed with 3 Rm C_{18} beads. Peptides were separated with a 120 min gradient (buffer A: 0.1% FA; buffer B: 0.1% FA in ACN) on an Easy-nLC system (ThermoFischer Scientific). The LC gradient started eluting from 5% buffer B to 40% buffer B in 90 min, increased to 95% buffer B in 5 min, and then remained eluting at 95% buffer B for 10 min. A Velos Orbitrap mass spectrometer (ThermoFisher Scientific) was used with a MS survey scan at a resolution of R=60,000, and the five most abundant peaks were selected with a mass window of 3 m/z units for MS/MS fragmentation in the Velos LTQ ion trap by collision-induced dissociation (CID) and electron transfer dissociation (ETD). Three technical replicate analyses of each FASP digested sample were performed, two of them with both CID and ETD MS/MS, and one analysis with only CID MS/MS. Therefore, only two of these technical replicates provided information about the presence of isoAsp. Finally, each in-gel digestion was analyzed by LC-MS once with both CID and ETD MS/MS.

Data processing

Peak list generation and database searches—MS/MS spectra were extracted, charge state deconvoluted and deisotoped using a home-written program RAW_to_MGF version 2.0.5, which also limited each MS/MS spectrum to its 200 most intense peaks. Then, MS/MS spectra from different runs were merged together using a home-written program Cluster_MGF to make one .MGF file for FASP digested samples and one .MGF file for in-gel digested samples. Cluster_MGF gathers groups of MS/MS spectra that share N of the 20 most-intense fragment peaks (N is usually 10). These groups are presumed to originate from MS/MS of the same peptide. The spectrum in each group that has the maximum aggregate intensity is taken as a representative of this group for storage in the .MGF file, while other MS/MS spectra are discarded.[28] This procedure greatly reduces the size of the resultant .MGF file and the time required for its subsequent matching to a MS/MS database performed by the Mascot search engine (Matrix Science, London, UK; version 2.3.02). The search was performed separately for CID and ETD MS/MS data, with a precursor mass window of 10 ppm, a MS/MS window of 0.6 Da, a maximum of two missed tryptic cleavages, and carbamidomethylation of cysteine as a fixed modification. Asparagine and glutamine deamidation and methionine oxidation were allowed as variable modifications (inclusion of these variable modifications made sequence assignment more reliable). The database search was performed against the UniProt_Complete_Proteomes_*Mus*_V_06-03-2013 database concatenated with decoy reverse-sequence compilation of this database for false discovery rate (FDR) determination (contains 42,793 sequences, plus an equal number of the reversed sequences).

Criteria for protein identification—Scaffold (version Scaffold_4.0.3, Proteome Software Inc., Portland, OR) was used to improve the accuracy of MS/MS-based peptide and protein identification. Peptide identification was accepted if it was deemed by the Scaffold Local FDR algorithm to be of greater than 95% reliability. Protein identification containing at least two identified peptides was accepted with a greater than 99% probability. Protein probabilities were assigned by the Protein Prophet algorithm.[29] Proteins that contained similar peptides and could not be differentiated based on MS/MS analysis alone were grouped to satisfy the principles of parsimony. Proteins sharing significant peptide evidence were pooled into clusters.

Protein quantification—Label-free quantification of the proteins was performed by the home-written program Quanti version 2.5.3.1.[28] This program integrates extracted ion chromatograms (XICs) of peptides identified by Mascot and considers all charge states and available isotopic peaks of the molecular ions. Quanti uses for quantification only reliably identified (FDR < 0.01), first-choice, unmodified, unique-sequence peptides. No less than two such peptides have to be present for a protein to be quantified. If two database protein entries have partial sequence overlap, then all the peptides belonging to this overlap are excluded from quantification.

Statistical analysis—The quantified proteome results were analyzed by SIMCA software (version 13.0.0.0, Umetrics AB, Sweden) performing principal component analysis (PCA).

Bioinformatic functional analysis—The functional analysis was performed using the DAVID (Database for Annotation, Visualization and Integrated Discovery, version 6.7) Bioinformatics Resource. Proteins identified as differentially expressed between control and PIMT-KO mice were assessed by Gene Ontology (GO) using significant enrichment of biological processes.

Isoaspartate identification and quantification—IsoAsp content was analyzed by the home-written software Isoaspartatics version 1.1.6, which looked for Asn deamidation and Asp isomerization by the presence of (z - 57 Da) ions in the ETD MS/MS spectra. Identification of an isoAsp site required that the (z - 57 Da) ion did not overlap with any theoretical m/z for c or z ions, and matched the expected mass with the tolerance of 0.1 Da. IsoAsp-containing peptides were quantified based on their extracted ion chromatograms, which required base-line chromatographic separation between the native and modified peptides. Additional criteria, like MS/MS identification of the native Asp form of the isoAsp-containing peptide and observation of the isotopic peak of the (z - 57 Da) ions, were applied to further substantiate the presence of an isoAsp residue.

Results

IsoAsp identification and quantification

Our first goal was to use mass spectrometry to identify proteins that contain isoAsp residues in WT mouse brains and in brain proteins from mice lacking the isoAsp-repair methyltransferase, PIMT. The presence of the signature (z - 57 Da) ions appears to be specific for identification of the subtle posttranslational modification (CH_2 group rearrangement from the side chain to the backbone) accompanying isoaspartyl formation.[16, 22] In the present study, we selected isoAsp-containing peptide candidates only if the peptides were successfully identified and quantified in all FASP digested samples, and the signature ion was present in both FASP digestion technical replicates. Using this stringent criterion, 67 unique isoAsp-containing peptides were detected. In peptides from PIMT-KO mouse brain proteins, 12 isoAsps originated at sites of asparagine deamidation

and 36 arose from the isomerization of aspartyl residues. In peptides from WT control brain proteins, 11 isoAsps originated at sites of asparagine deamidation and 33 arose from the isomerization of aspartyl residues. Nine of the 14 isoAsp sites resulting from deamidation were common to proteins from both WT and PIMT-KO animals, and 16 of the 53 isoAsp sites generated by aspartyl residue isomerization were found in both WT and KO brains (Tables S2 – S5). The absence of the repair methyltransferase in PIMT-KO mouse brain has previously been shown to result in an accumulation of isoAsp residues, and 23 sites of isoAsp formation were found here solely in the PIMT-KO mouse brain proteins. Surprisingly, however, an additional 19 unique isoAsp sites were found in WT but not KO brain proteins. The appearance of isoAsp sites in WT but not in KO mice could be a spurious result of insufficient statistics in isoAsp detection by MS/MS. The difference between the isoAsp spectral counts in PIMT-KO and WT mice, although in favor of PIMT-KO, was too small to be statistically significant. Thus, an alternative to MS/MS spectral counting method was needed to assess the relative isoAsp levels in these groups.

In principle, the Quanti program is capable of quantifying all of the variants of each peptide in the dataset. However, this required reliable chromatographic separation between the native and isoAsp peptides, which was not always the case. Since the main goal was to assess the general isoAsp level in PIMT-KO and WT brains, while individual peptide data were less important, we selected as representative two peptides with well-separated chromatograms and reliable MS/MS identification of both native and isoAsp-containing peptides, and the presence of the isotopic distribution of the (z - 57 Da) ion. The relative abundances of the variants were quantified by their XICs.

After quantification, the difference between the PIMT KO and WT mice became more apparent. Among the 19 isoAsp sites uniquely identified by MS/MS in WT mice, none of the 17 peptides with isomerization-induced isoAsps (which to a higher degree than deamidation-generated isoAsps are due to *in vivo* accumulation) showed significantly different levels in WT vs KO. At the same time, among the 23 sites unique for KO mouse, two out of 20 isomerization-induced isoAsp sites (Table S6) showed high significance ($p < 0.001$): LDLIAQQMMPEVR from V-type proton ATPase subunit E1 (the KO/WT abundance ratio = 1.29) and VDNDENEHQLSLR from nucleophosmin (the KO/WT abundance ratio = 1.32).

Even more apparent was the difference among the levels of peptides with isoAsp detected by MS/MS in both types of mice, or only in KO mice. To demonstrate this difference, we chose two peptides with chromatographically well-separated isoAsp and native variants; the ratio of abundances of these variants provided the estimate for the isoAsp occupancy. The measurements of occupancies (stoichiometries) made with two replicate proteomic analyses of each of the eight mice (four mice of each type) allowed for reliable statistical evaluation of the results.

The two investigated peptides were ^{92}VFDKDG**N**GYISAAEL^{107}R from calmodulin (Figure 1) and ^{65}LVI**N**GKPITIFQE^{78}R from glyceraldehyde-3-phosphate dehydrogenase (Figure 2). The relatively large amount of isoAsp observed in the peptides generated from the WT mouse proteins suggests that these Asn residues are particularly labile and may have deamidated during the proteolytic digestion and processing. The larger relative abundance of isoAsp residues in the comparable peptides from PIMT-KO proteins, however, indicates how much of these sites might be repaired by PIMT *in vivo*. The isoAsp occupancy of ^{92}VFDKDG**N**GYISAAEL^{107}R in PIMT-KO mice was almost two times the amount in WT controls ($p < 0.01$ in two-tailed Student's t-test) (Figure 3A). Zero counts in Figure 3 correspond to the cases when the quantification program could not reliably attribute any XIC in the LC/MS dataset to the corresponding peptide. The isoAsp occupancy

of ^{65}LVI**N**GKPITIFQE^{78}R in PIMT-KO mice was somewhat more than two times that in WT controls ($p < 0.001$ in two-tailed Student's t-test) (Figure 3B). Here, the average abundance ratio of isoAsp and Asp variants is 4.6 for PIMT KO and 3.6 for WT mice, which is consistent with isoAsp repair by PIMT and its conversion to Asp. The quantification data for these two modified peptides are given in Table S7.

Protein identification and quantification by FASP

Although it is likely that the increase in isoAsp levels in PIMT-KO mice contributes to the observed phenotype, it remains unclear what other cellular changes might be contributing to this phenotype. To determine whether expression levels of critical proteins were altered by the absence of PIMT, we identified by the FASP method 5768 peptides belonging to 832 proteins with an FDR < 1% (Tables S8 and S9), and were able to quantify 811 of these proteins (Table S10). Two-dimensional PCA analysis (SIMCA, $R^2X[cum]=0.912$; $Q^2[cum]=0.785$) successfully separates this dataset into two groups: WT controls and PIMT-KO mice (Figure 4). Then two-tailed Student's t-test was applied to select the proteins that were significantly altered in PIMT-KO compared to WT controls. The threshold p-value was chosen to be $p < 0.001$; thus, less than one false significant protein was expected in the whole dataset containing 811 proteins. The analysis resulted in 182 significantly altered proteins (Table S11), including PIMT that was found as the 725th most abundant protein in WT samples and absent in PIMT KO mice (Figure S1).

Protein identification and quantification by in-gel digestion

To validate the results found with the FASP method described above, we next used a different protein preparation technique, gel-based separation and in-gel digestion, to generate peptides for MS analysis. In total, 4628 unique peptides belonging to 796 proteins were identified with an FDR <1% (Tables S12 and S13). With a minimum of two unique peptides, 790 of these proteins were quantified (Table S14). Although in-gel digestion provides less accurate data than FASP in label-free quantification due to multiple steps involving protein or peptide losses, PCA analysis was still able to separate the two groups of mice (Figure S2 A). Most of the significantly regulated proteins found in FASP (90%) were also quantified using the in-gel digested sample. Among the 163 significantly regulated proteins quantified by both methods, 151 proteins (93%) had the same regulation direction in both analyses (Table S15, Figure S2 B and C). Using $p < 0.005$ as a significance cut-off threshold for the in-gel method (for 151 proteins, $p < 0.005$ guarantees on average less than one false significant protein), the most reliably identified significantly regulated proteins were determined (Table 1).

Bioinformatic functional analysis

Our final goal here was to determine what specific changes in protein levels observed in the PIMT-KO mouse brain could contribute to the phenotype observed in these mice. Among the most reliable 151 significant proteins (Table S15), 83 are up-regulated in PIMT-KO mice, and 68 down-regulated. Using all identified proteins as a background dataset (Table S16) and $p < 0.001$ as a significance threshold, Gene Ontology (GO) analysis was performed. Analysis of proteins down-regulated in PIMT-KO mice yielded cellular amino acid biosynthesis as the only significantly enriched process ($p = 0.0008$). Thus this process is likely to be suppressed in PIMT-KO brains compared to WT. Up-regulated in PIMT-KO mice proteins did not yield any process with statistical significance.

Discussion

Isoaspartome regulated by PIMT

Protein deamidation and isomerization are spontaneous reactions both *in vitro* and *in vivo*. The reaction rates for these modifications are influenced by the primary sequence and three-dimensional structure, as well as by the temperature, pH and ionic strength of the solution. Therefore, the *in vitro* deamidation rate can be approximately predicted *in silico* using a computational model built with help of extensive experimental data.[30] In the pharmaceutical industry, minimizing deamidation and isomerization during drug production, formulation and storage is of great importance.[31] Under physiological conditions, isoAsp residues arising at specific sites by deamidation and isomerization can have regulatory functions, such as in the response to DNA damage[32] and in p53 stability.[12] High isoAsp levels have negative impact in mammalian tissues; e.g., they can affect the crystal structure of human lens[33] and induce an autoimmune response.[34] Therefore, isoAsp formation and PIMT repair capability have essential roles in both cellular regulation and protein ageing processes.

Until recently, isoAsp identification and quantitation has mostly been carried out by the ISOQUANT® Isoaspartate Detection Kit, which uses recombinant PIMT to radiolabel isoAsp residues with S-adenosyl-[3H-methyl]-methionine.[35] Two recent reports use this assay, combined with 2D electrophoresis and blotting on membranes, to isolate isoAsp containing proteins from PIMT-KO mouse brains.[7, 11] When methylation was performed first, followed by electrophoresis, blotting, and MS, 12 isoAsp-containing proteins were identified,[7] though this technique might have lost the most labile methyl esters during the purification procedure.[36] When the enzymatic methylation was instead performed after the proteins had been separated and blotted onto a membrane, 19 isoAsp-containing proteins were identified,[11] though some of these isoAsps may be new non-physiological sites that were generated during the procedure. The difference between these procedures is illustrated by the fact that only alpha- and beta-tubulin were identified in both reports as containing isoAsp residues. In contrast to these previous reports, we have used the recent discovery of a specific (z - 57 Da) fragment ion of isoAsp in ECD/ETD MS/MS spectra[21] and the procedures described in this current study to detect a total of 67 isoAsp containing proteins. Four of the 12 isoAsp-containing proteins found by Vigneswara et al.,[7] including clathrin light chain a and calmodulin, and 9 of the 19 isoAsp-containing proteins found by Zhu et al.,[11] including synapsins I and II, are confirmed here, and now we have identified a specific site of damage in each of these proteins.

The fact that we observed three-times more isoAsp residues in WT and PIMT-KO proteins arising from aspartyl isomerization than from asparaginyl deamidation is quite surprising. In one previous report, the rates of isoAsp formation measured *in vitro* in small synthetic peptides were found to be 6.5- to 21-times faster at Asn sites than from the corresponding Asp sites at 37 °C, pH 7.4.[37] Our results here support the idea that isoAsp formation from Asn deamidation is limited by native protein structure in the mouse brain, while isoAsp formation from Asp isomerization is perhaps promoted by the structure of these proteins. In addition to identifying labile asparaginyl and aspartyl residues in mouse brain proteins, we also wanted to know which sites are repaired by PIMT within brain cells. When repair is occurring, the isoAsp occupancy at a particular site will be lower in the WT brain than in the PIMT-KO brain. This will be observed even if deamidation during the experimental procedure generates new isoAsp residues, because in vitro deamidation will occur equally in the PIMT-KO and WT proteins. Rather than using the enzymatic assay, the amount of isoAsp can now be quantified by specific fragment abundance,[38] counts of MS/MS spectra containing the signature fragment,[18] targeted multiple reaction monitoring (MRM) assay,[23] or by label-free quantification based on XIC.[22] In the present study, we used XIC to

quantify two isoAsp-containing peptides which have clear base-line chromatographic separation between the native and isoAsp variants and excellent MS/MS data.

The peptide ^{92}VFDKDG**N**GYISAAEL^{107}R containing isoAsp-98 originates from calmodulin, located in the calcium binding loop of the EF hand (domain III). Calmodulin contains four EF hand domains, and each of the domains can bind calcium. Interestingly, the domain with Asn-98 has the highest calcium binding affinity among all domains.[39] The transformation of Asn-98 to Asp-98 or isoAsp-98 in calmodulin results in loss of 60% and 90% protein activity, respectively.[2] Detection of isoAsp-98 is not surprising: Asn-98 was found to be the most susceptible site for isoAsp formation during *in vitro* protein ageing.[39] Previously, only low levels of isoAsp had been identified in calmodulin from PIMT-KO mouse brains.[10] Although much of the isoAsp we observe at this labile site may have arisen during *in vitro* processing, the differences in PIMT-KO vs WT isoAsp levels between these studies may reflect the different efficiencies of the two techniques of isoAsp quantification for this specific deamidation site of calmodulin. Almost twice as much isoAsp was found in this calcium-binding domain in PIMT-KO compared to WT mice. Lower calcium-binding activity of isoAsp-containing calmodulin molecules may disturb the downstream calmodulin-dependent pathways.

Another peptide with a higher isoAsp level in PIMT-KO mice, ^{65}LVI**N**GKPITIFQE^{78}R containing isoAsp-68, belongs to glyceraldehyde-3-phosphate dehydrogenase (GAPDH). To our knowledge, this is the first time that GAPDH has been identified as an *in vivo* substrate for PIMT. GAPDH is an important housekeeping enzyme, and its involvement in glycolysis has been well-studied. Other biological functions, such as membrane fusion, have also been associated with GAPDH.[40] In *in vitro* experiments, the main deamidation site of GAPDH has been localized in the N-terminal peptide (^{2}VKVGVNGFG^{11}R), where the structure is quite constrained.[41] Asn-68 has not been reported previously as a major deamidation site. The domain which contains peptide ^{65}LVI**N**GKPITIFQE^{78}R has no known catalytic activity, but it can bind tryptophanyl-tRNA synthetase.[42] This domain can also contribute to the membrane fusion function.[40] The biological effects of deamidation of Asn-68 in GAPDH are unclear, but may result in the reduction of the above functions.

As described above for calmodulin, the true isoAsp levels in both proteins are likely to be somewhat lower than measured due to the almost inevitable *in vitro* deamidation occurring during sample preparation. This artifact is relatively more important for WT mice, where isoAsp levels are lower. Therefore, the true isoAsp occupancy change due to the absence of repair in PIMT-KO cells is likely to be much higher than the factor of two obtained here, and thus closer to the factor of six measured in crude mouse brain preparations in the previous study by enzymatic methylation.[5]

The altered proteome and pathways

Although all of the new isoAsp sites discovered here will need to be quantitated and their effect on protein function assayed to determine their specific role in mouse brain cell function, we can also examine their cumulative effect on cellular metabolism by examining how protein expression levels are altered in PIMT-KO cells. The four proteins with most significantly altered expression levels (two up-regulated and two down-regulated) are given in Table 1.

The protein CAMKV (CaM kinase-like vesicle-associated protein) that is up-regulated 1.8- to 2.7-fold in PIMT-KO mice is considered catalytically inactive, but it may, according to UniProt, play a role in vesicle function and nervous system development. One proteomic study on the Ercc1 mouse model, which has DNA repair deficiency and thus exhibits accelerated ageing, has reported significant up-regulation of this protein.[43] As CAMKV

shares sequence similarities with Ca^{2+}/calmodulin-dependent protein kinase (CaMK), it could also be important for Ca^{2+} homeostasis.

The protein GLSK (glutaminase, kidney isoform) is up-regulated in PIMT-KO mice as well (1.4- to 1.9 fold). Both the kidney isoform (GLSK or GLS1) and liver isoform (GLS2) of glutaminase are expressed in the brain.[44] Glutaminase catalyzes the conversion of glutamine to glutamate. Glutamate is one of the main neurotransmitters, and 70% of the glutamate used in neurotransmission is generated through the glutamine-glutamate pathway with the help of GLSK.[45] Although GLSK-knockout is fatal for mice, glutamatergic synaptic transmission in cultured GLSK-KO cortical neurons is normal. Therefore, compensating minor glutamate-generating pathways seem to be present in neurons, such as transamination of α-ketoglutarate with alanine, branched-chain amino acids or lysine, that maintain glutamatergic synaptic transmission.[45]

PCBP2 (Poly(rC)-binding protein 2), down-regulated 0.7- to 0.8-fold in PIMT-KO mice, is essential for mRNA stability and translational controls (silencing and enrichment).[46] PCBP2 is also involved in innate immunity acting as a negative regulator in MAVS-mediated antiviral signaling. The expression of PCBP2 is significantly altered upon viral infection.[47] As down-regulation of PCBP2 is also found in hepatitis C virus (HCV)-replicon containing cells (R1b), it is thought to have an antiviral effect for HCV.[48] Moreover, PCBP2 has an important role in stress response by binding with MAPKAP1 (mitogen-activated protein kinase associated protein 1).[49] Cells with down-regulation of either MAPKAP1 or PCBP2 are more susceptible to environmental stress, such as viral infection, inflammation shock, or oxidative stress.[49] Therefore, such a down-regulation of PCBP2 protein expression could reflect a weakened stress-responding system in PIMT-KO mice.

Another protein that is down-regulated (0.8-fold) in PIMT-KO mice is DX39B (spliceosome RNA helicase Ddx39b). DX39B is important for pre-RNA splicing and mRNA exportation from nucleus to cytoplasm.[50] The suppression of DX39B expression by RNAi causes the accumulation of a majority of the mRNAs inside the nucleus.[51] In cardiomyocytes, the presence of DX39B and ATPase are essential for protein synthesis.[52] The down-regulation of DX39B that perturbs the mRNA expression process may contribute to the smaller-size of the PIMT-KO mice,[4] as suggested before.[53]

In order to investigate which biological networks are most affected by PIMT knockout, the DAVID bioinformatics tool was used in mapping the 151 significantly regulated proteins (Table S15) to the Gene Ontology categories. The cellular amino acid biosynthetic process (GO: 0008652) was enriched with proteins down-regulated in PIMT-KO mice ($p = 0.0008$). Among these proteins, glutamine synthetase (GLNA) is involved in glutamine generation; aspartate aminotransferase (AATC) - in glutamate oxidation; excitatory amino acid transporter 1 (EAAT1) - in glutamate transportation; D-3-phosphoglycerate dehydrogenase (SERA) and phosphoserine aminotransferase (SERC) - in serine biosynthesis.

At this point, it becomes apparent that the glutamate-glutamine cycle in CNS is significantly disturbed in PIMT-KO mice, which agrees well with previous knowledge.[5] Glutamate is the major excitatory neurotransmitter. After pre-synaptic release, the majority of glutamate is transported via EAAT1 into astrocytes, where glutamate is converted into glutamine via GLNA (Figure 5).[54] Then glutamine is transported back into the neurons, and converted into glutamate via GLSK. At the same time, brain oxidizes glutamate via AATC, continuously generating aspartate and 2-oxo-glutarate.[55] In PIMT-KO mice, we observed down-regulation of EAAT1, GLNA and AATC, but up-regulation of GLSK. The net effects should be an increase in the level of glutamate, which is consistent with the previous observations of 30% more glutamate in synaptosomes of PIMT-KO mice.[5] Excessive

glutamate excitatory signals have been associated with epilepsy,[56] thus the dysregulated glutamate-glutamine cycle may account for the epileptic seizures and, subsequently, of untimely death of PIMT-KO mice.

SERA and SERC are the first two enzymes involved in the serine synthesis pathway, which is the primary source of serine biosynthesis in the brain.[57] Serine is mainly produced in astrocytes, and has an essential role in CNS function and development.[57] Besides being consumed in protein synthesis, serine is used for generation of glycine and the neurotransmitter D-serine, as well as several neuronal membrane lipids.[57] Serine deficiency causes intractable seizures in patients.[57] A high level of serine synthesis has been found in some cancer cell lines and is associated with breast cancer.[58] Serine is also the main carbon donor, via homocysteine to S-adenosylmethionine, of methylation reactions.[59] Therefore, the down-regulation of serine synthesis enzymes might significantly affect the one-carbon methylation metabolism in PIMT-KO mice. In fact, this down-regulation could possibly be compensating for the increased S-adenosylmethionine and decreased S-adenosylhomocysteine that is observed in PIMT-KO mouse brains. Further investigation of this hypothesis, however, is needed.

Conclusions

Here we confirmed the ability of modern proteomics to investigate simultaneously the isoaspartome and the protein expression levels using a standard, high-throughput, untargeted, label-free proteomics experiment. Overall 67 novel as well as previously known isoAsp-containing sites were identified, and two sites were thoroughly quantified, providing additional verification of significant isoAsp accumulation in the PIMT-deficient brain. The biological effects of isoAsp accumulation in each of the identified proteins remain to be further investigated. The expression levels of a large number of quantified proteins (ca. 15%) were found to be significantly altered when compared to WT levels, suggesting large changes in the global brain proteome. GO mapping of the proteins with altered levels verify the earlier finding that glutamate metabolism is a main metabolic process perturbed with PIMT deficiency, supporting possible regulatory roles of that enzyme. Additional findings, that require further validation, indicate that PIMT mice may suffer from serine deficiency.

Supplementary Material

Refer to Web version on PubMed Central for supplementary material.

Acknowledgments

This work was supported by the Knut and Alice Wallenberg Foundation, VINNOVA Foundation, Alzheimersfonden, the Swedish Research Council, and National Institutes of Health (grant GM026020).

References

1. Clarke S. Aging as war between chemical and biochemical processes: protein methylation and the recognition of age-damaged proteins for repair. Ageing Res Rev. 2003; 2 (3):263–85. [PubMed: 12726775]
2. Johnson BA, Langmack EL, Aswad DW. Partial repair of deamidation-damaged calmodulin by protein carboxyl methyltransferase. J Biol Chem. 1987; 262 (25):12283–7. [PubMed: 3624258]
3. Johnson BA, Murray ED Jr, Clarke S, Glass DB, Aswad DW. Protein carboxyl methyltransferase facilitates conversion of atypical L- isoaspartyl peptides to normal L-aspartyl peptides. J Biol Chem. 1987; 262 (12):5622–9. [PubMed: 3571226]
4. O'Connor, CM. Protein L-isoaspartyl, D-aspartyl O-methyltransferases: catalysts for protein repair. In: Steven, GC.; Fuyuhiko, T., editors. The Enzymes. Vol. 24. Academic Press; 2006. p. 385-433.

5. Kim E, Lowenson JD, MacLaren DC, Clarke S, Young SG. Deficiency of a protein-repair enzyme results in the accumulation of altered proteins, retardation of growth, and fatal seizures in mice. Proc Natl Acad Sci US A. 1997; 94 (12):6132–7.
6. Yamamoto A, Takagi H, Kitamura D, Tatsuoka H, Nakano H, Kawano H, Kuroyanagi H, Yahagi Y, Kobayashi S, Koizumi K, Sakai T, Saito K, Chiba T, Kawamura K, Suzuki K, Watanabe T, Mori H, Shirasawa T. Deficiency in protein L-Isoaspartyl methyltransferase results in a fatal progressive epilepsy. J Neurosci. 1998; 18 (6):2063–74. [PubMed: 9482793]
7. Vigneswara V, Lowenson JD, Powell CD, Thakur M, Bailey K, Clarke S, Ray DE, Carter WG. Proteomic identification of novel substrates of a protein isoaspartyl methyltransferase repair enzyme. J Biol Chem. 2006; 281 (43):32619–29. [PubMed: 16923807]
8. Lanthier J, Bouthillier A, Lapointe M, Demeule M, Béliveau R, Desrosiers RR. Down-regulation of protein l-isoaspartyl methyltransferase in human epileptic hippocampus contributes to generation of damaged tubulin. J Neurochem. 2002; 83 (3):581–91. [PubMed: 12390520]
9. Young GW, Hoofring SA, Mamula MJ, Doyle HA, Bunick GJ, Hu Y, Aswad DW. Protein L-Isoaspartyl methyltransferase catalyzes in vivo racemization of aspartate-25 in mammalian histone H2B. J Biol Chem. 2005; 280 (28):26094–8. [PubMed: 15908425]
10. Reissner KJ, Paranandi MV, Luc TM, Doyle HA, Mamula MJ, Lowenson JD, Aswad DW. Synapsin I is a major endogenous substrate for protein L-Isoaspartyl methyltransferase in mammalian brain. J Biol Chem. 2006; 281 (13):8389–98. [PubMed: 16443604]
11. Zhu JX, Doyle HA, Mamula MJ, Aswad DW. Protein repair in the brain, proteomic analysis of endogenous substrates for protein L-isoaspartyl methyltransferase in mouse brain. J Biol Chem. 2006; 281 (44):33802–13. [PubMed: 16959769]
12. Lee JC, Kang SU, Jeon Y, Park JW, You JS, Ha SW, Bae N, Lubec G, Kwon SH, Lee JS, Cho EJ, Han JW. Protein L-isoaspartyl methyltransferase regulates p53 activity. Nat Commun. 2012; 3:927.10.1038/ncomms1933 [PubMed: 22735455]
13. Farrar C, Houser CR, Clarke S. Activation of the PI3K/Akt signal transduction pathway and increased levels of insulin receptor in protein repair-deficient mice. Aging Cell. 2005; 4 (1):1–12. [PubMed: 15659208]
14. MacKay KB, Lowenson JD, Clarke SG. Wortmannin reduces insulin signaling and death in seizure-prone Pcmt$^{-/-}$ mice. PLoS One. 2012; 7(10)10.1371/journal.pone.0046719
15. Kosugi S, Furuchi T, Katane M, Sekine M, Shirasawa T, Homma H. Suppression of protein lisoaspartyl (D-aspartyl) methyltransferase results in hyperactivation of EGF-stimulated MEK-ERK signaling in cultured mammalian cells. Biochem Biophys Res Commun. 2008; 371 (1):22–7. [PubMed: 18381200]
16. Yang H, Lyutvinskiy Y, Soininen H, Zubarev RA. Alzheimer's disease and mild cognitive impairment are associated with elevated levels of isoaspartyl residues in blood plasma proteins. J Alzheimers Dis. 2011; 27 (1):113–8. [PubMed: 21765210]
17. Yang H, Wittnam JL, Zubarev RA, Bayer TA. Shotgun brain proteomics reveals early molecular signature in presymptomatic mouse model of Alzheimer's disease. J Alzheimers Dis. 2013 accepted.
18. Wiśniewski JR, Ostasiewicz P, Mann M. High recovery FASP applied to the proteomic analysis of microdissected formalin fixed paraffin embedded cancer tissues retrieves known colon cancer markers. J Proteome Res. 2011; 10 (7):3040–9. [PubMed: 21526778]
19. Fischer F, Wolters D, Rogner M, Poetsch A. Toward the complete membrane proteome - High coverage of integral membrane proteins through transmembrane peptide detection. Mol Cell Proteomics. 2006; 5 (3):444–53. [PubMed: 16291997]
20. Yang H, Zubarev RA. Mass spectrometric analysis of asparagine deamidation and aspartate isomerization in polypeptides. Electrophoresis. 2010; 31 (11):1764–72. [PubMed: 20446295]
21. Cournoyer JJ, Pittman JL, Ivleva VB, Fallows E, Waskell L, Costello CE, O'Connor PB. Deamidation: Differentiation of aspartyl from isoaspartyl products in peptides by electron capture dissociation. Protein Sci. 2005; 14 (2):452–63. [PubMed: 15659375]
22. Yang H, Fung EYM, Zubarev AR, Zubarev RA. Toward proteome-scale identification and quantification of isoaspartyl residues in biological samples. J Proteome Res. 2009; 8 (10):4615–21. [PubMed: 19663459]

23. Dai SJ, Ni WQ, Patananan AN, Clarke SG, Karger BL, Zhou ZS. Integrated proteomic analysis of major isoaspartyl-containing proteins in the urine of wild type and protein L-isoaspartate Omethyltransferase- deficient mice. Anal Chem. 2013; 85 (4):2423–30. [PubMed: 23327623]
24. Geiger T, Clarke S. Deamidation, isomerization, and racemization at asparaginyl and aspartyl residues in peptides. Succinimide-linked reactions that contribute to protein degradation. J Biol Chem. 1987; 262 (2):785–94. [PubMed: 3805008]
25. Li XJ, Cournoyer JJ, Lin C, O'Connor PB. Use of O-18 labels to monitor deamidation during protein and peptide sample processing. J Am Soc Mass Spectrom. 2008; 19(6):855–864. [PubMed: 18394920]
26. Du Y, Wang FQ, May K, Xu W, Liu HC. Determination of deamidation artifacts introduced by sample preparation using O-18-labeling and tandem mass spectrometry analysis. Anal Chem. 2012; 84(15):6355–6360. [PubMed: 22881398]
27. Liu HC, Wang FQ, Xu W, May K, Richardson D. Quantitation of asparagine deamidation by isotope labeling and liquid chromatography coupled with mass spectrometry analysis. Anal Biochem. 2013; 432(1):16–22. [PubMed: 23017877]
28. Lyutvinskiy Y, Yang H, Rutishauser D, Zubarev RA. In silico instrumental response correction improves precision of label-free proteomics and accuracy of proteomics-based predictive models. Mol Cell Proteomics. 201310.1074/mcp.O112.023804
29. Nesvizhskii AI, Keller A, Kolker E, Aebersold R. A statistical model for identifying proteins by tandem mass spectrometry. Anal Chem. 2003; 75 (17):4646–58. [PubMed: 14632076]
30. Robinson NE, Robinson AB. Deamidation of human proteins. Proc Natl Acad Sci US A. 2001; 98 (22):12409–13.
31. Wakankar AA, Borchardt RT. Formulation considerations for proteins susceptible to asparagine deamidation and aspartate isomerization. J Pharm Sci. 2006; 95 (11):2321–36. [PubMed: 16960822]
32. Deverman BE, Cook BL, Manson SR, Niederhoff RA, Langer EM, Rosov I, Kulans LA, Fu X, Weinberg JS, Heinecke JW, Roth KA, Weintraub SJ. Bcl-xL deamidation is a critical switch in the regulation of the response to DNA damage. Cell. 2002; 111 (1):51–62. [PubMed: 12372300]
33. Takata T, Oxford JT, Demeler B, Lampi KJ. Deamidation destabilizes and triggers aggregation of a lens protein, beta A3-crystallin. Protein Sci. 2008; 17 (9):1565–75. [PubMed: 18567786]
34. Eggleton P, Haigh R, Winyard PG. Consequence of neo-antigenicity of the 'altered self'. Rheumatology. 2008; 47 (5):567–71. [PubMed: 18316337]
35. Johnson BA, Shirokawa JM, Hancock WS, Spellman MW, Basa LJ, Aswad DW. Formation of isoaspartate at two distinct sites during in vitro aging of human growth hormone. J Biol Chem. 1989; 264 (24):14262–71. [PubMed: 2760065]
36. Morrison GJ, Ganesan R, Qin Z, Aswad DW. Considerations in the identification of endogenous substrates for protein L-isoaspartyl methyltransferase: The case of synuclein. PLoS One. 2012; 7(8)10.1371/journal.pone.0043288
37. Stephenson RC, Clarke S. Succinimide formation from aspartyl and asparaginyl peptides as a model for the spontaneous degradation of proteins. J Biol Chem. 1989; 264 (11):6164–70. [PubMed: 2703484]
38. Cournoyer JJ, Lin C, Bowman MJ, O'Connor PB. Quantitating the relative abundance of isoaspartyl residues in deamidated proteins by electron capture dissociation. J Am Soc Mass Spectrom. 2007; 18 (1):48–56. [PubMed: 16997569]
39. Potter SM, Henzel WJ, Aswad DW. In vitro aging of calmodulin generates isoaspartate at multiple Asn–Gly and Asp–Gly sites in calcium-binding domains II, III, and IV. Protein Sci. 1993; 2 (10): 1648–63. [PubMed: 8251940]
40. Daubenberger CA, Tisdale EJ, Curcic M, Diaz D, Silvie O, Mazier D, Eling W, Bohrmann B, Matile H, Pluschke G. The N′-terminal domain of glyceraldehyde-3-phosphate dehydrogenase of the apicomplexan Plasmodium falciparum mediates GTPase Rab2-dependent recruitment to membranes. Biol Chem. 2003; 384 (8):1227–37. [PubMed: 12974391]
41. Rivers J, McDonald L, Edwards IJ, Beynon RJ. Asparagine deamidation and the role of higher order protein structure. J Proteome Res. 2008; 7 (3):921–7. [PubMed: 18247555]

42. Filonenko VV, Beresten SF, Rubikaite BI, Kisselev LL. Bovine tryptophanyl-tRNA synthetase and glyceraldehyde-3-phosphate dehydrogenase form a complex. Biochem Biophys Res Commun. 1989; 161 (2):481–8. [PubMed: 2735904]
43. Vegh MJ, de Waard MC, van der Pluijm I, Ridwan Y, Sassen MJM, van Nierop P, van der Schors RC, Li KW, Hoeijmakers JHJ, Smit AB, van Kesteren RE. Synaptic proteome changes in a DNA repair deficient Ercc1 mouse model of accelerated aging. J Proteome Res. 2012; 11 (3):1855–67. [PubMed: 22289077]
44. Olalla, La; Gutiérrez, A.; Campos, JA.; Khan, ZU.; Alonso, FJ.; Segura, JA.; Márquez, J.; Aledo, JC. Nuclear localization of L-type glutaminase in mammalian brain. J Biol Chem. 2002; 277 (41): 38939–44. [PubMed: 12163477]
45. Masson J, Darmon M, Conjard A, Chuhma N, Ropert N, Thoby-Brisson M, Foutz AS, Parrot S, Miller GM, Jorisch R, Polan J, Hamon M, Hen R, Rayport S. Mice lacking brain/kidney phosphate-activated glutaminase have impaired glutamatergic synaptic transmission, altered breathing, disorganized goal-directed behavior and die shortly after birth. J Neurosci. 2006; 26 (17):4660–71. [PubMed: 16641247]
46. Makeyev AV, Liebhaber SA. The poly(C)-binding proteins: A multiplicity of functions and a search for mechanisms. RNA. 2002; 8 (3):265–78. [PubMed: 12003487]
47. You F, Sun H, Zhou X, Sun W, Liang S, Zhai Z, Jiang Z. PCBP2 mediates degradation of the adaptor MAVS via the HECT ubiquitin ligase AIP4. Nat Immunol. 2009; 10 (12):1300–8. [PubMed: 19881509]
48. Xin Z, Han W, Zhao Z, Xia Q, Yin B, Yuan J, Peng X. PCBP2 Enhances the antiviral activity of IFN-α against HCV by stabilizing the mRNA of STAT1 and STAT2. PLoS One. 2011; 6(10)10.1371/journal.pone.0025419
49. Ghosh D, Srivastava GP, Xu D, Schulz LC, Roberts RM. A link between SIN1 (MAPKAP1) and poly(rC) binding protein 2 (PCBP2) in counteracting environmental stress. Proc Natl Acad Sci US A. 2008; 105 (33):11673–8.
50. Shi H, Cordin O, Minder CM, Linder P, Xu RM. Crystal structure of the human ATPdependent splicing and export factor UAP56. Proc Natl Acad Sci US A. 2004; 101 (51):17628–33.
51. Herold A, Teixeira L, Izaurralde E. Genome-wide analysis of nuclear mRNA export pathways in Drosophila. Embo J. 2003; 22 (10):2472–83. [PubMed: 12743041]
52. Sahni A, Wang N, Alexis JD. UAP56 is an important regulator of protein synthesis and growth in cardiomyocytes. Biochem Biophys Res Commun. 2010; 393 (1):106–10. [PubMed: 20116367]
53. Farrar CE, Clarke S. Diet-dependent survival of protein repair-deficient mice. J Nutr Biochem. 2005; 16 (9):554–61. [PubMed: 16115544]
54. Fillenz M. Physiological release of excitatory amino acids. Behav Brain Res. 1995; 71 (1–2):51–67. [PubMed: 8747174]
55. Daikhin Y, Yudkoff M. Compartmentation of brain glutamate metabolism in neurons and glia. J Nutr. 2000; 130 (4):1026–31.
56. Meldrum BS. The role of glutamate in epilepsy and other CNS disorders. Neurology. 1994; 44 (11 Suppl 8):S14–23. [PubMed: 7970002]
57. Tabatabaie L, Klomp LW, Berger R, de Koning TJ. l-Serine synthesis in the central nervous system: A review on serine deficiency disorders. Mol Genet Metab. 2010; 99 (3):256–62. [PubMed: 19963421]
58. Kalhan SC, Hanson RW. Resurgence of serine: An often neglected but indispensable amino acid. J Biol Chem. 2012; 287 (24):19786–91. [PubMed: 22566694]
59. Davis SR, Stacpoole PW, Williamson J, Kick LS, Quinlivan EP, Coats BS, Shane B, Bailey LB, Gregory JF. Tracer-derived total and folate-dependent homocysteine remethylation and synthesis rates in humans indicate that serine is the main one-carbon donor. Am J Physiol Endocrinol Metab. 2004; 286 (2):E272–9. [PubMed: 14559726]

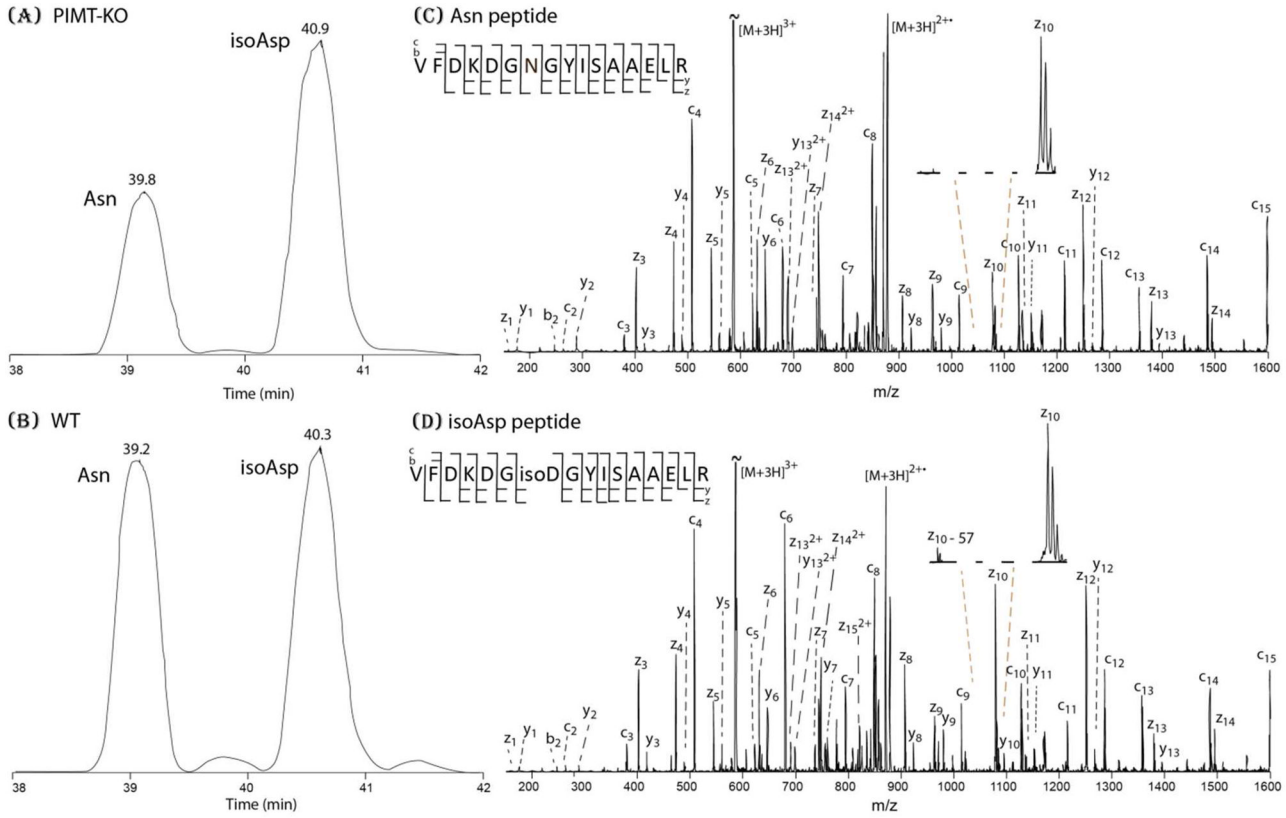

Figure 1.

Left: Extracted ion chromatographic profiles of 3+ ions of peptide ^{92}VFDKDG**N**GYISAAEL^{107}R (Asn) from calmodulin and its deamidated form ^{92}VFDKDG**isoD**GYISAAEL^{107}R (isoAsp). **A**: PIMT KO mice. **B**: WT mice. **Right**: ETD MS/MS spectrum of 3+ ions. **C:** ^{92}VFDKDG**N**GYISAAEL^{107}R (Asn) native peptide. **D**: ^{92}VFDKDG**isoD**GYISAAEL^{107}R (isoAsp) peptide. Insert shows the absence or presence of (z – 57 Da) ions.

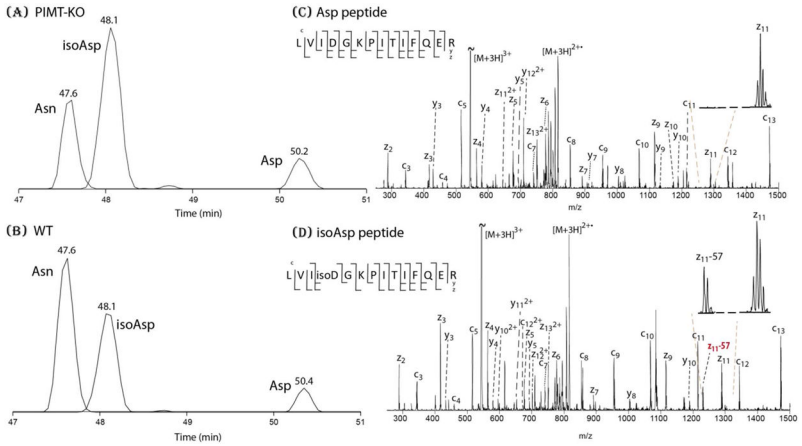

Figure 2.

Left: Extracted ion chromatographic profiles of 3+ ions of peptide ^{65}LVI**N**GKPITIFQE^{78}R (Asn) from glyceraldehyde-3-phosphate dehydrogenase and its deamidated forms ^{65}LVI**D**GKPITIFQE^{78}R (isoAsp) and ^{65}LVI**D**GKPITIFQE^{78}R (Asp) in the samples of **A:** PIMT KO mice and **B:** WT mice. **Right**: ETD MS/MS spectrum of 3+ ions of **C:** the ^{65}LVI**D**GKPITIFQE^{78}R (Asp) peptide. **D**: the ^{65}LVI**isoD**GKPITIFQE^{78}R (isoAsp) peptide. Insert shows the absence or presence of (z – 57 Da) ions.

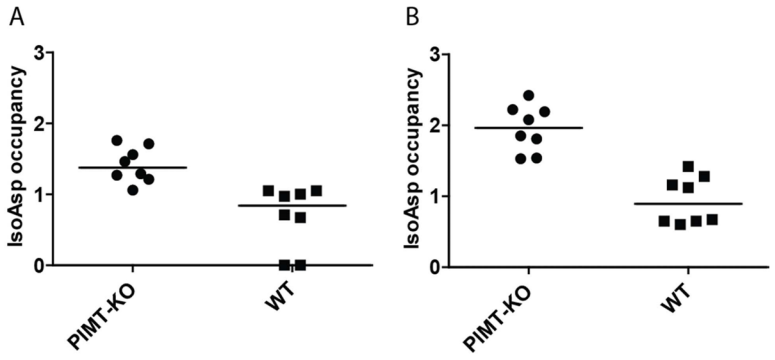

Figure 3.

A: IsoAsp occupancy (ratio of the isoAsp/native peptide abundances) in the calmodulin peptide VFDKDG**N**GYISAAELR (**Panel A**) and and the glyceraldehyde-3-phosphate dehydrogenase peptide LVI**N**GKPITIFQER (**Panel B**) in four PIMT-KO mice and four WT controls measured in two replicate FASP-based proteomic analyses. Lines indicate the median value in each dataset.

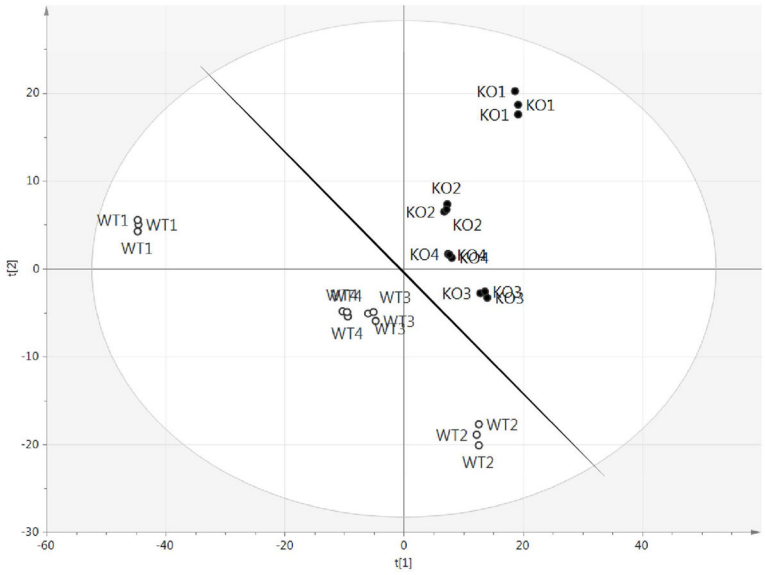

Figure 4.

Principal component analysis (PCA) of protein abundances from the whole-brain proteome analysis performed by FASP digestion (SIMCA, $R^2X[cum]=0.912$; $Q^2[cum]=0.785$): black circles (KO) - PIMT-KO mice; white circles (WT) - wild type controls. The line separates the dataset into two groups, PIMT-KO and WT.

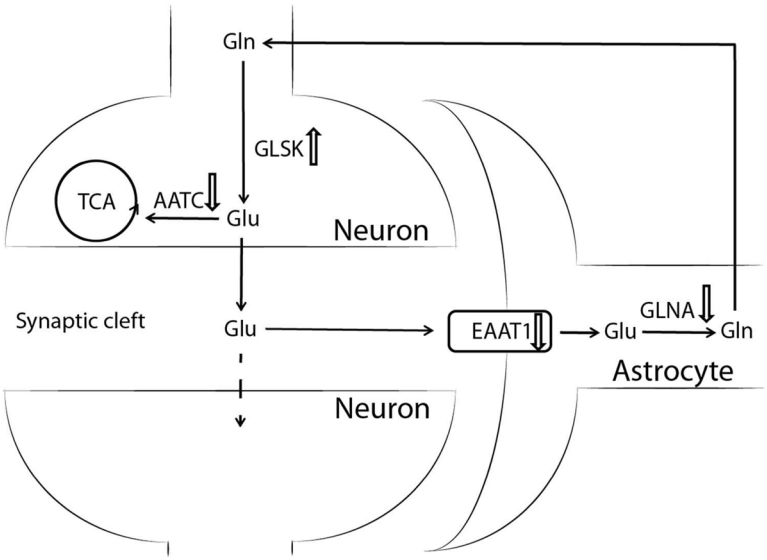

Figure 5.

Glutamate-glutamine cycle in the central nervous system. Glutamate (Glu) is synthesized from glutamine (Gln) by glutaminase (GLSK) in the pre-synaptic neurons and released into the synaptic cleft. Besides being taking up by the post-synaptic neurons, the majority of Glu is transported by excitatory amino acid transporters (EAAT) into nearby astrocytes, where it is converted into Gln by glutamine synthetase (GLNA). Then Gln is released by astrocytes into the extracellular matrix and taken up by neurons, where it re-enters the cycle. At the same time, Glu can be oxidized into a-ketoglutarate and enter the tricarboxylic acid (TCA) cycle via aspartate aminotransferase (AATC). The arrows by the protein names show their up- or down-regulation found in the current experiment. Figure adapted from Daikhin *et al.* (2000).[55]

Table 1

Proteins whose expression levels are significantly altered by the absence of the isoaspartyl methyltransferase in PIMT-KO mice compared to WT controls as found by both FASP ($p < 0.001$) and in-gel ($p < 0.005$) methods of proteomic analysis.

Protein ID	Description	FASP		In-gel	
		p value	fold KO/WT	p value	fold KO/WT
CAMKV_MOUSE	CaM kinase-like vesicle-associated protein	4.01E-04	1.8	3.37E-04	2.7
GLSK_MOUSE	Glutaminase, kidney isoform l	7.13E-09	1.4	1.29E-03	1.9
PCBP2_MOUSE	Poly(rC)-binding protein 2	9.15E-05	0.8	3.01E-03	0.7
DX39B_MOUSE	Spliceosome RNA helicase	4.01E-04	0.8	4.75E-03	0.8